Variational Mode Spectrum Estimation for Wire Rope Defect Inspection Signals Analysis and Quantitative Evaluation

SHIWEI LIU, YONG LIU, QIAOHUA WANG and WEIGUO LIN

Shwei Liu (Corresponding Author, E-mail: liusw@hzau.edu.cn), Yong Liu, Qiaohua Wang and Weiguo Lin are all with College of Engineering, Huazhong Agricultural University, No.1, Shizishan Street, Hongshan District, Wuhan, Hubei Province, 430070, P. R. China.

ABSTRACT

Wire rope is one of the most significant parts in guaranteeing the safety and health of infrastructures and practical structures. However, the defect frequently occurs when the wire rope is operating under sophisticated conditions, which makes the servicing wire rope and its related structures full of risk. Although many nondestructive testing techniques have been considered to solve the defect inspection and structural health monitoring (SHM) problems for wire rope, the inspection and monitoring results are greatly influenced by the testing environments. To deal with the challenges of quantitative wire rope nondestructive evaluation and SHM, a new variational mode decomposition and spectrum estimation method is proposed here. The preliminary signal analysis for typical wire broken defects under different wire rope operating speed is conducted in time, frequency and statistical domain. Then, a new quantitative wire rope evaluation method based on different defect signals features analysis, principle introduction, spectrum estimation and comparison with other mode decomposition techniques is presented, which demonstrate the feasibility and application promise for wire rope SHM and accurate evaluation.

INTRODUCTION

Wire rope is widely applied in various practical applications, such as the harbor, bridge, elevator, mine and energy exploration related fields, which is playing a significant role in guaranteeing the safety of infrastructures and human lives. However, the defect frequently occurs when the wire rope is operating under sophisticated conditions [1], such as the impact, shock, fatigue, wear and corrosion. Consequently, the local fault (LF) including the wire broken, crack and loss of metallic area (LMA) damage such as the surface wear have become the main forms of wire rope defect, which makes the servicing wire rope and its related structures full of risk [2]. Consequently, wire rope defect detection and health state monitoring are the key to ensure safety. Although various nondestructive testing method including the magnetic flux leakage testing [3], infrared thermography imaging [4] and machine vision-based techniques [5] are applied to defect inspection and structural health monitoring (SHM) problems [6] for wire rope, the inspection and monitoring results are greatly influenced by the interference of the surrounding environment, wire rope structures and operating conditions. Thus, a plenty of signal processing and pattern recognition methods [7] are proposed and reported, such as the time-frequency transform [8], wavelet denoising [9], image recognition [10], nonlinear mode decomposition [11, 12] and spectrum estimation [13], as well as machine learning and deep learning methods [14]. However, most of these methods are invalid for online wire rope signal processing when the wire rope defect inspection signals resemble to each other and small sample data is limited. To solve these challenges above, and quantitatively evaluate wire rope working condition, a new variational mode spectrum estimation for wire rope defect signal recognition method is proposed here, which has great potential of wire rope health monitoring in practical applications.

SIGNAL ANALYSIS

Four groups of typical wire rope testing signals labeled as s1 to s4 are obtained and shown in Figure 1, where a magnetic flux leakage testing detector is applied to sense two continuous broken wires with the nominal diameter of Φ 32 mm and single wire diameter of Φ 1.5 mm. Specifically, these inspection signals are acquired under the online rotating wire rope, which is driven by a motor and frequency converter, and the rotating frequency is set as 5 Hz, 10Hz, 15Hz and 20Hz for s1 to s4, separately.

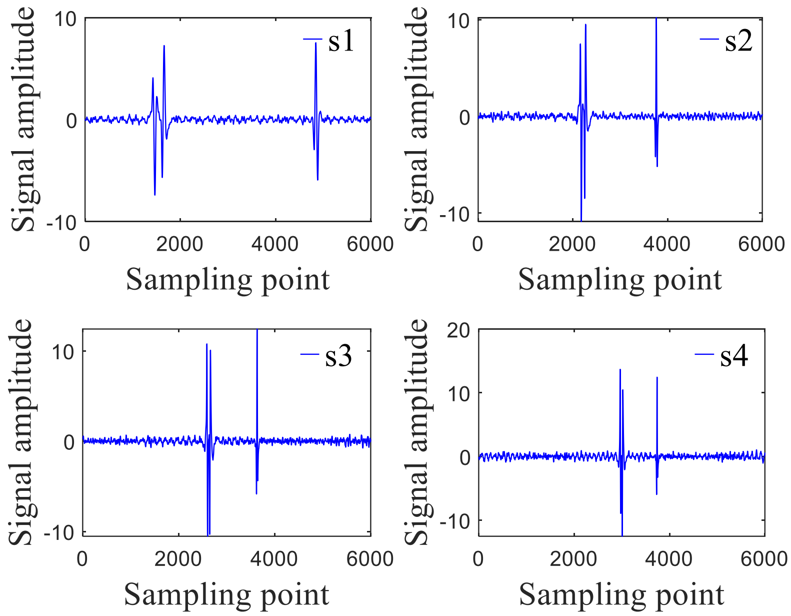

Figure 1. Typical wire rope defect inspection signals of s1 to s4.

It can be seen from these time series signals expressed in Figure 1 that, all of these defect inspection signals are featured with two similar prominent longitudinal mutation peaks, and its usually hard to distinguish these signals and their working conditions just by their amplitudes. Further three-dimensional (3D) spectrum analysis for s1 to s4 from the perspective of frequency, phase and amplitude domain is illustrated in Figure 2, and it can also be noted that almost all these four signals have semblable features in phase, frequency and amplitude. In other words, it's almost impossible to identify these similar defect inspection signals just by the time domain characterizations.

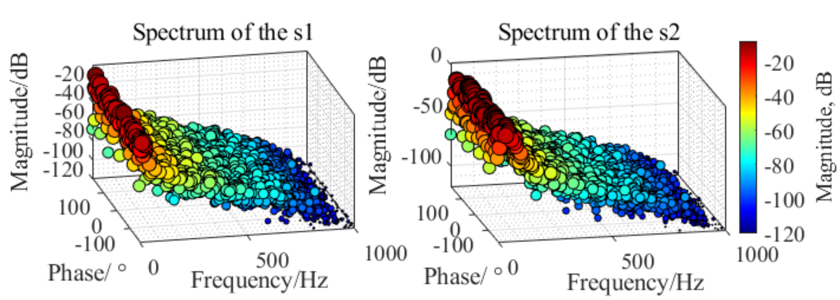

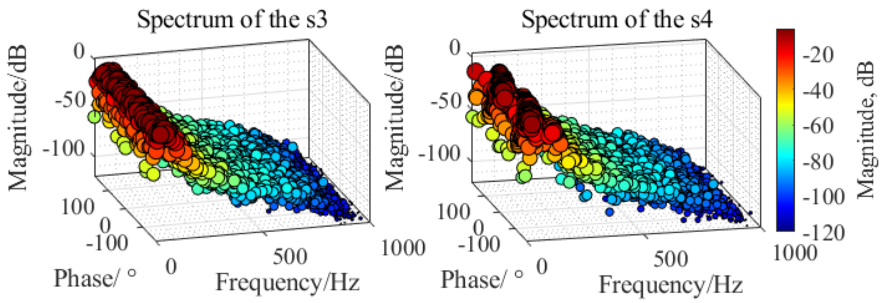

Figure 2. 3D spectrum analysis for wire rope testing signals of s1 to s4.

Besides, further kernel density estimation for these four signals is also conducted and the results are presented in Figure 3, where s1 to s4 are analyzed from the perspective of statistics. However, after calculating these signals, we can preliminarily find that all these signals are analogously distributed in the two-dimensional (2D) plane, which are all expressed as accumulation areas around the central position of (0, 0). As the kernel density increases, all the signals are attenuated in amplitude, and s1 to s4 are closely resemble to each other and presented as an approximate 2D normal distribution.

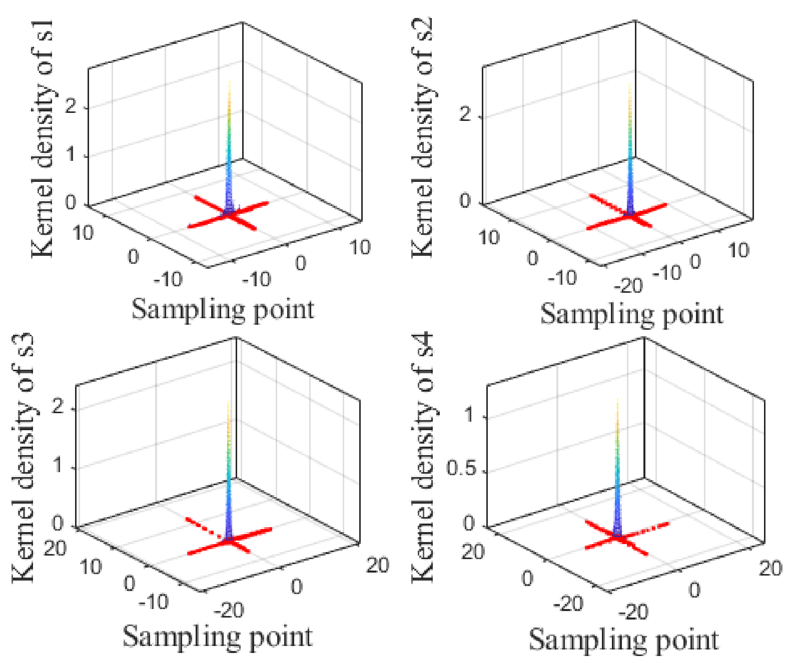

Figure 3. Kernel density estimation for s1 to s4.

Owing to that the operating speed or driven frequency of the wire rope is very close which may lead to the defect detection signal frequency diverse, the fast Fourier transform (FFT) and power spectral density (PSD) calculation results for s1 to s4 are also obtained and given in Figure 4. Primarily, the single-sided amplitude spectrum of FFT and the frequency response of PSD are presented. All these signals are distributed within the frequency band lower than 500Hz, and most of them are gathered near 0 to 100 Hz. What's more, it's still difficult to find obvious difference among s1 to s4 in frequency domain by the calculating results shown in Figure 4.

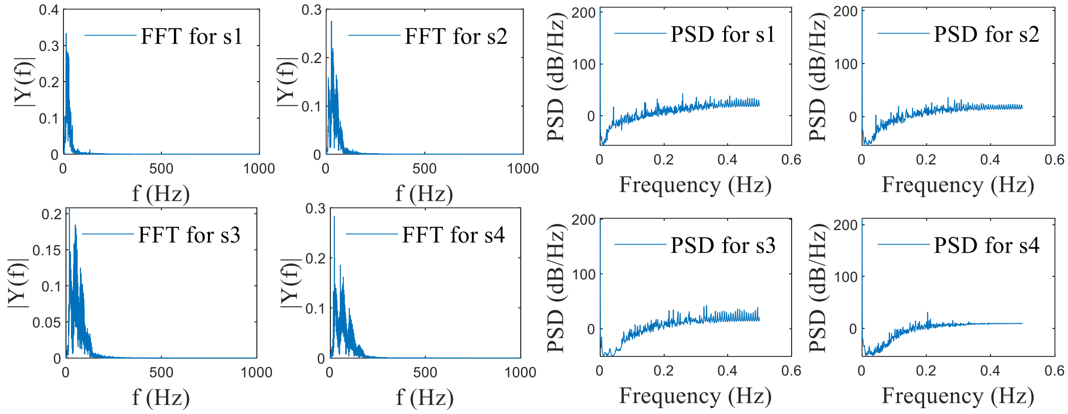

Figure 4. Signal analysis results of FFT and PSD for s1 to s4.

Therefore, another statistical analysis method for these original wire rope testing signals through feature extraction is presented, where the 10 main features describing different defect inspection conditions including the enhanced mean absolute value (EMAV), average amplitude change (AAC), waveform length (WL), maximum fractal length (MFL), enhanced wave length (EWL), kurtosis (KURT), skewness (SKEW), slope sign change (SSC), zeros crossing (ZC), log detector (LD) are investigated, and the calculating results are expressed in Table I.

TABLE I. TEN MAIN EIGENVALUES OF WIRE ROPE TESTING SIGNAL

Feature	EMAV	AAC	WL	MFL	EWL	KURT	SKEW	ZC	SSC	LD
s1	0.4188	0.0295	177.2405	0.7460	542.9872	31.5024	0.2985	150.00	146.00	0.1371
s2	0.3966	0.0389	233.6235	0.9963	621.3383	59.5609	0.7390	204.00	179.00	0.1249
s3	0.4029	0.0505	303.2779	1.1280	744.0274	74.3039	2.2312	310.00	326.00	0.1370
s4	0.4683	0.0614	368.2151	1.2008	861.2379	86.6561	3.0103	281.00	436.00	0.1886

Although these eigenvalues are different in numerical values, it's usually impossible to identify their operation conditions just by the single feature. As the pattern recognition techniques including the machine learning and deep learning neural network fast develop, they have been prevalently applied in the wire rope defect inspection, but a more lightweight and less data-dependent method for wire rope working conditions monitoring and evaluation is still lacked and desperately needed.

VARIATIONAL MODE SPECTRUM ESTIMATION

According to the decomposition principle of variational mode decomposition (VMD) [15], the wire rope testing signal $y(t)$ is decomposed as several accumulation of intrinsic mode functions (IMFs) of $s_k(t)$, which can be expressed as the product of an amplitude of $A_k(t)$ and the component of $\cos(\phi_k(t))$,

$$s_k(t) = A_k(t)\cos(\phi_k(t)) \tag{1}$$

Where, k is the decomposed mode number, $\phi_k(t)$ is the signal envelope, and the constraints of the narrow band distributed wire rope inspection signals are described as,

$$\begin{cases} \min\limits_{\{s_k\}\{\omega_k\}} \{\sum_{k=1}^{K} \left\| \partial_t [(\delta(t) + \frac{j}{\pi t}) * s_k(t)] e^{-j\omega_k t} \right\|_2^2 \} \\ s.t. \quad \sum_{k=1}^{K} s_k(t) = y(t) \end{cases} \tag{2}$$

To solve the above problem, an augmented Lagrangian function is built as,

$$L(\{s_k\},\{\omega_k\},\lambda) = \alpha \sum_{k=1}^{K} \left\| \partial_t [(\delta(t) + \frac{j}{\pi t}) * s_k(t)] e^{-j\omega_k t} \right\|_2^2 + \left\| y(t) - \sum_{k=1}^{K} s_k(t) \right\|_2^2 + \left\langle \lambda(t), y(t) - \sum_{k=1}^{K} s_k(t) \right\rangle \tag{3}$$

Where, α is the penalty coefficient, λ is the Lagrangian multiplier. Then, the alternate direction method of multipliers and the Parseval theorem in frequency domain are considered to calculate the final results of the decomposed signal as,

$$\mathrm{s}_k^{n+1} = \arg\min_{s_k} L(\{s_{i<k}^{n+1}\},\{\omega_k^n\},\lambda^n) \tag{4}$$

$$\omega_k^{n+1} = \arg\min_{\omega_k} L(\{s_k^{n+1}\},\{\omega_{i<k}^n\},\lambda^n) \tag{5}$$

$$\lambda^{n+1} = \lambda^n + \rho(y(t) - \sum_{k=1}^{K} s_k^{n+1}(t)) \tag{6}$$

Owing to that the 1D wire rope signal analysis in the single time and frequency domain are difficult in identifying their working conditions especially when these signals are semblable, a 2D signal spectrum estimation method is proposed through the VMD characterization, and the detailed VMD for wire rope signals is presented in Algorithm 1.

Algorithm 1 Quantitative wire rope evaluation by VMD spectrum estimation
Step 1 Parameter initialization; **Step 2** 1D signal reconstructed as a 2D matrix; **Step 3** Compute the halfplane mask for the 2D signal; **Step 4** Update first mode accumulator, spectrum and central frequency; **Step 5** Recover full spectrum from the original signal; **Step 6** Gradient ascent for augmented Lagrangian function mentioned in (3); **Step 7** Repeat Step 3 to Step 6 until the maximum iteration is reached; **Step 8** Signal reconstruction through inverse Fourier transform to compute each mode; **Step 9** Return the decomposition modes and spectrum; **Step 10** Estimate the spectrum enhancement area and build the quantitative mathematical relationships evaluating the wire rope working conditions; **Step 11** Obtain the quantitative wire rope evaluation results.

Explanatorily, the balancing parameter for data fidelity constraint, the decomposition mode number, tolerance of convergence criterion and other parameters are first initialized, then 1D original wire rope testing signals are reconstructed as a 2D matrix and input of the variational mode decomposition procedure. What's more, the first mode's VMD spectrum is updated through a wiener filter and its central frequency is updated as the spectral center of gravity, meanwhile, the gradient ascent is applied to solve the Lagrangian function mentioned in (3). Finally, the inverse Fourier transform processed and the mode decomposed signals are reconstructed as a mode spectrum, where the spectrum estimated enhancement regions are used to build the quantitative wire rope evaluation model. Consequently, the mode decomposed spectrum of the original wire rope testing signals of s1 to s4, especially for the first VMD component of mode 1 is presented in Figure 5.

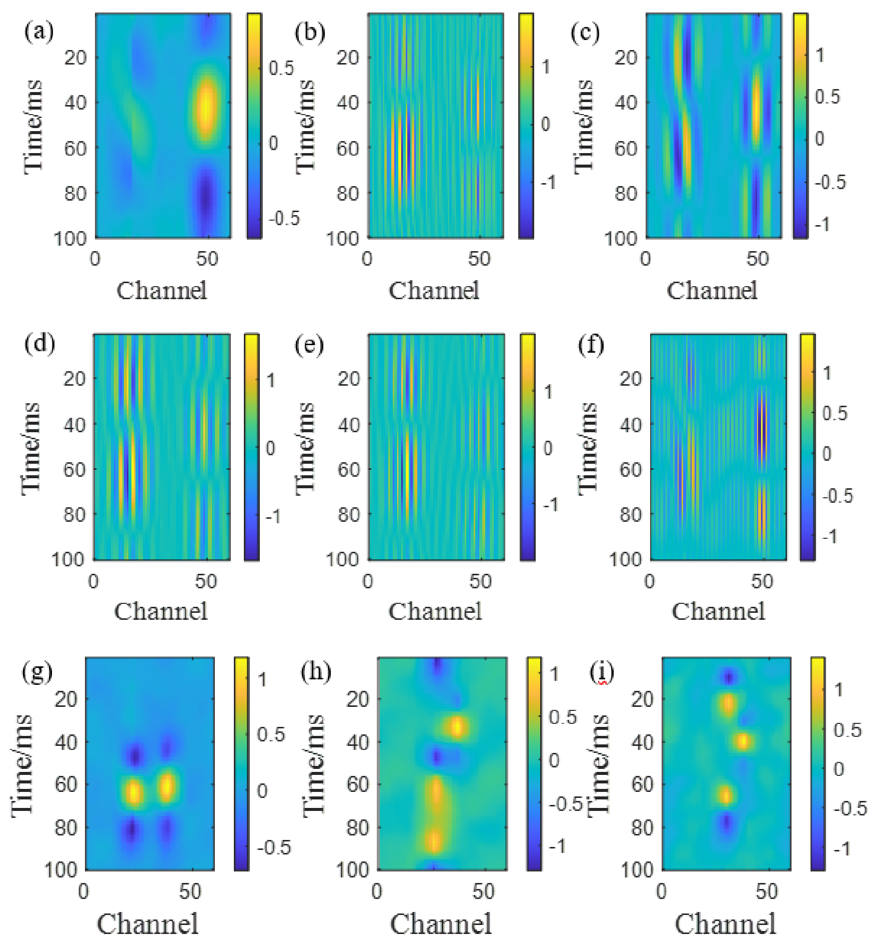

Figure 5. Mode decomposition spectrum of s1 to s4. (a) Mode 1 of s1; (b) Mode 2 of s1; (c) Mode 3 of s1; (d) Mode 4 of s1; (e) Mode 5 of s1; (f) Mode 6 of s1; (g) Mode 1 of s2; (h) Mode 1 of s3; (i) Mode 1 of s4.

It can be seen from Figure 5 that there is only one spectrum enhancement region for mode 1 of s1, and 2, 3, 3 strengthened areas for s2 to s4. As for mode 2 to mode 6 decomposed from s1 shown in Figure 5(b) to 5(f), these spectrum stripes resemble among different modes. Afterwards, the mode 1 for s1 to s4 are mainly considered to realize the working condition identification. Besides, comparing these 2D mode spectrums of s1 to s4 with that of the original signals shown in Figure 1, it can be found that although all these signals have two prominent signal peaks and similar characterizations both in time and frequency domain, they can be possibly distinguished by the spectrum differences especially by the decomposed time judged by the longitudinal value and spectrum enhancement region. Therefore, another groups of wire rope testing signals are further investigated, and the typical testing samples of T1, T2 and T3 are obtained when the inspection wire rope is operating under the frequency converter parameter of 25 Hz, 35Hz and 40Hz, separately. Similarly, the original signals of T1 to T3 and their corresponding VMD spectrum calculated through the decomposed mode 1 are illustrated in Figure 6. Obviously, although these signals are still likewise in amplitude, their spectrums are differently distributed, where 3, 4 and 6 spectrum enhancement areas in yellow color are respectively appeared. Combining the spectrum information mentioned for s1 and s6, a quantitative wire rope working condition evaluation model for the frequency converter driving parameter or the wire rope operating speed can be preliminarily built.

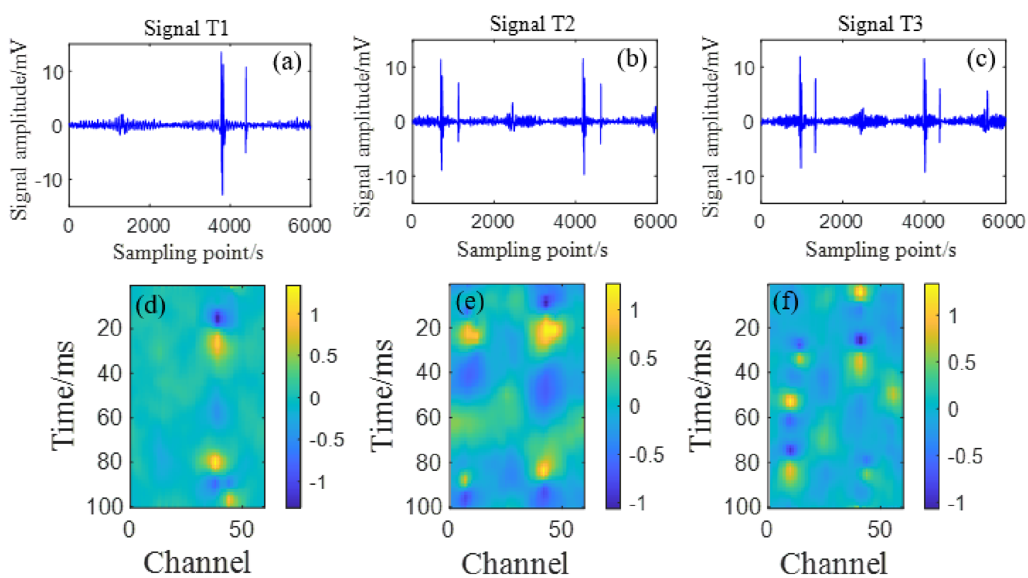

Figure 6. Mode 1 of signal T1 to T3. (a) Signal T1; (b) Signal T2; (c) Signal T3; (d) Mode 1 of T1; (e) Mode 2 of T1; (f) Mode 3 of T1.

According to the calculating results mentioned above, the relationships between the wire rope working condition and the total VMD spectrum enhancement region number is presented in Figure 7(a), where a positively related curves between these two parameters can be found. Besides, to exactly described their quantitative relationships, the weighted number combining the spectrum enhancement region and corresponding channel is defined as,

$$W = \sum_{i=1}^{5} \frac{n_i E_i}{N} \tag{7}$$

Where, E_i is the channel zone of the enhanced spectrum from 10 to 50 with a step of 10, n_i is the enhanced spectrum distributed within each channel zone, N is the total spectrum enhancement region number. Consequently, the relationship between W and the wire rope operating speed characterized by the frequency of x can be expressed as a polynomial model of (8), Where, x is the frequency converter driving frequency or the wire rope operating speed, and the calculated and polynomial function fitted relationships between x and $W(x)$ are expressed in Figure 7(b).

$$W(x) = 0.0002x^5 - 0.0103x^4 + 0.2959x^3 - 4.0005x^2 + 21.3998x + 11.9841 \quad (8)$$

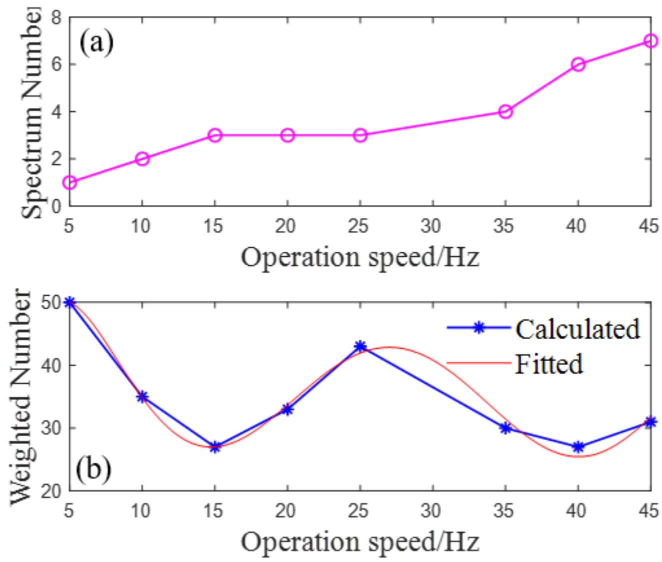

Figure 7. Quantitative relationship between wire rope operation speed and the VMD spectrum enhancement area number. (a) Operation speed with total VMD spectrum enhancement region number; (b) Operation speed with weighted number.

Combining Figure 7(a) and the quantitative relationships mentioned in (8), the wire rope working conditions can be exactly monitored just by the defect inspection signals for online rotating wire ropes.

COMPARISON AND QUANTITATIVE EVALUATION

To further validate the feasibility of the quantitative wire rope evaluation method, T-50 signals acquired under the rotating frequency of 50Hz is considered, and the original signal of T-50 and the VMD spectrum of mode 1 is presented in Figure 8.

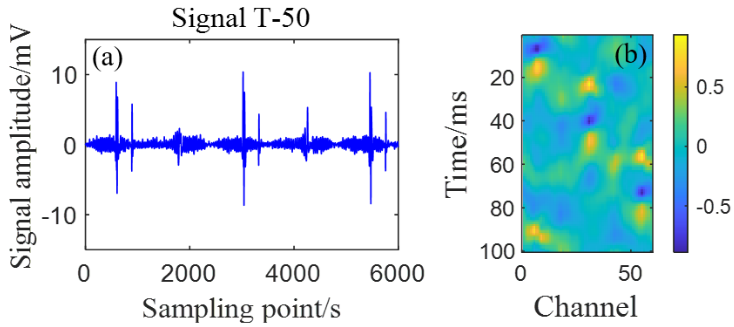

Figure 8. Testing results for T-50 by the new method. (a) Signal of T-50; (b) Mode 1 spectrum for T-50.

There are totally 8 approximate enhancement areas and the weighted number of 31.25. Let W(x) = 31.25, then combing the positive relationships expressed in Figure 7(a), we can obtain that the solution of x = 49.9749. Namely, the absolute error with the accurate frequency of 50 is 0.0251 Hz, and the relative error is 0.050113%. Additionally, the calculating results of decomposed mode analysis for T-50 through empirical mode decomposition (EMD) [11] and the reported variational nonlinear chirp mode decomposition (VNCMD) methods [12] are presented in Figure 9. Comparing with the proposed method mentioned in Figure 8, the signal enhancement areas calculated through EMD and VNCMD are all consistent with the original time series signal of T-50, which manifests that the EMD and VNCMD are incapable of recognizing the working condition and differentiating different wire rope defect signals, while the proposed VMD spectrum features estimation method provides a quantitative evaluation strategy.

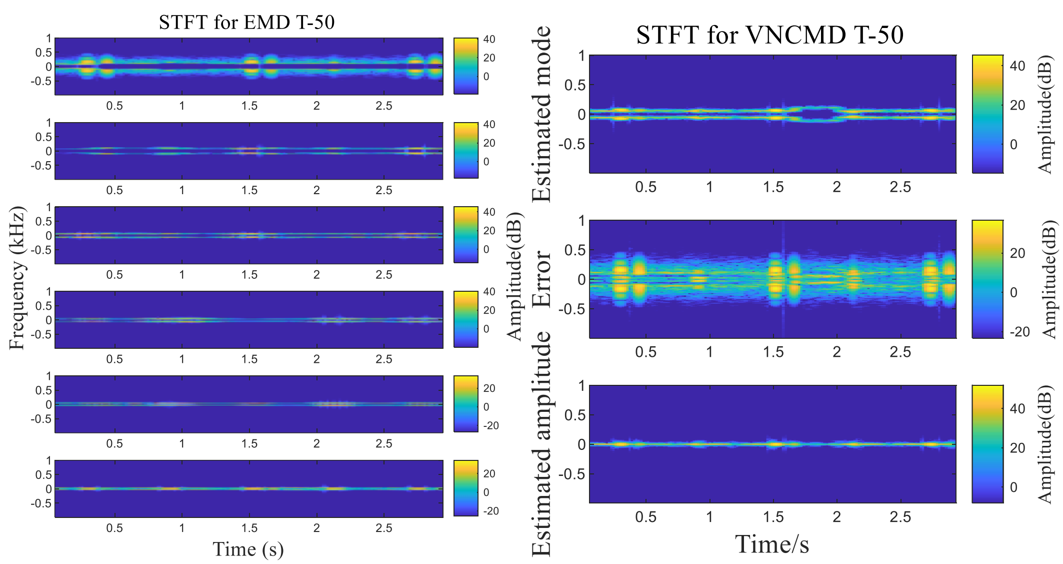

Figure 9. STFT for EMD and VNCMD testing results of and T-50.

CONCLUSION

(1) Typical wire rope defect inspection signals are investigated from the perspective of time domain, frequency domain and statistics, which manifest that the common

methods are difficult to recognize their working conditions when these defect signals resemble to each other.

(2) A new VMD spectrum estimation method is proposed for quantitative evaluation where the mathematical modeling and comparing results demonstrate the feasibility and validity of the method, which is potentially to be widely applied in wire rope defect inspection and health monitoring.

REFERENCES

1. Zhao D, Liu S, Xu Q, et al. "Fatigue life prediction of wire rope based on stress field intensity method," *Engineering Failure Analysis*, 2017, 81: 1-9.
2. Liu S, Sun Y, Jiang X, et al. "A review of wire rope detection methods, sensors and signal processing techniques," *Journal of Nondestructive Evaluation*, 2020, 39: 1-18.
3. Kim J W, Park S. "Magnetic flux leakage–based local damage detection and quantification for steel wire rope non-destructive evaluation," *Journal of Intelligent Material Systems and Structures*, 2018, 29(17): 3396-3410.
4. Heinz D, Halek B, Krešák J, et al. "Methodology of measurement of steel ropes by infrared technology," *Engineering Failure Analysis*, 2022, 133: 105978.
5. Lee W, Cao K. Application of Machine Vision to Inspect a Wiring Harness[C]//*2019 IEEE International Conference on Industrial Cyber Physical Systems (ICPS)*. IEEE, 2019: 457-460.
6. Witoś M, Zieja M, Fallahi N, et al. "NDE and SHM of critical parts using magnetic and electromagnetic methods," *Acta Physica Polonica A*, 2018, 133(3): 697-700.
7. Kim J W, Tola K D, Tran D Q, et al. "MFL-based local damage diagnosis and SVM-based damage type classification for wire rope NDE," *Materials*, 2019, 12(18): 2894.
8. Zhang Y, Xu K, Zang J, et al. "Dynamic design of a nonlinear energy sink with NiTiNOL-steel wire ropes based on nonlinear output frequency response functions," *Applied Mathematics and Mechanics*, 2019, 40(12): 1791-1804.
9. Liu S, Sun Y, Ma W, et al. "A new signal processing method based on notch filtering and wavelet denoising in wire rope inspection," *Journal of Nondestructive Evaluation*, 2019, 38: 1-14.
10. Tan X, Zhang J. "Evaluation of composite wire ropes using unsaturated magnetic excitation and reconstruction image with super-resolution," *Applied Sciences*, 2018, 8(5): 767.
11. Zhang J, Zheng P, Tan X. "Recognition of broken wire rope based on remanence using EEMD and wavelet methods," *Sensors*, 2018, 18(4): 1110.
12. Chen S, Dong X, Peng Z, et al, "Nonlinear Chirp Mode Decomposition: A Variational Method," *IEEE Transactions on Signal Processing*, 2017.
13. Zosso D, Dragomiretskiy K, Bertozzi A L, et al. "Two-dimensional compact variational mode decomposition: Spatially compact and spectrally sparse image decomposition and segmentation," *Journal of Mathematical Imaging and Vision*, 2017, 58: 294-320.
14. Zhang Y, Feng Z, Shi S, et al. "A quantitative identification method based on CWT and CNN for external and inner broken wires of steel wire ropes," *Heliyon*, 2022, 8(11): e11623.
15. K. Dragomiretskiy, D. Zosso, "Variational Mode Decomposition," *IEEE Trans.on Signal Processing*, 62(3):531-544, 2014.